pairing occurs between aromatic organic cations and inorganic anions. If the temperature range used to obtain the apparent activation energies in this study was such that, as the temperature is increased, the equilibria between loose and tighter ion pairs is shifted toward an increase in tighter ion pairs, then the line width observed would increase or at least not decrease by the amount expected. The plot of log k *vs.* $1/T$ would then give a lower slope and thus a lower apparent activation energy. The small temperature range used in this study could prevent the change in sign of d log k/d$(1/T)$, as was observed by the workers in ref 7 and 13, from being detected unambiguously.

Our results would imply that the concentration ratios of different ion pairs do not change rapidly enough with temperature to change the sign of the apparent activation energy, but the anomalous behavior in the log k *vs.* $1/T$ plot would give low activation energy values.

Summary and Conclusion

We have determined the second-order rate constants for the ($TPTA^+$) and ($PTAZ^+$) exchanging cation systems in the region of fast exchange in various solvent mixtures. It was found that the rate constants were solvent dependent (except for iodine oxidized ($TPTA^+$) systems). The rate constant dependence on the dielectric constant of the solvent has been attributed to ion pairing between the organic aromatic cation and inorganic anion present. Steric factors which prevent formation of various types of ion pairs in the ($TPTA^+$–I^-) system have been invoked to rationalize the solvent independence of the rate constants obtained for this system.

The anomalous activation energies obtained for systems having extensive ion pairing have been attributed to a shift in equilibria between various types of ion pairs with temperature.

Organic reactions which proceed *via* an ion-pair intermediate mechanism have been reported.[41] In such reactions attention must be given to the possible types of ion pairs that can result. We have shown in this study that the structure of the species involved in making ion pairs greatly affects the resulting ion pair and in some instances prevents ion pair formation. Structural consideration of the ion pair intermediate should not be overlooked when studying organic reactions which proceed *via* such mechanisms.

Acknowledgment is made to donors of the Petroleum Research Fund, administered by the American Chemical Society, for partial support of this research. A generous allotment of computer time made available to S. P. S by the Lincoln Computing Facility of the University of Nebraska Computer Network is also gratefully acknowledged. Acknowledgment is also made to Dr. C. J. Michejda, University of Nebraska, for discussions and advice.

(41) (a) R. A. Sneen and J. W. Larsen, *J. Amer. Chem. Soc.*, **91**, 6031 (1969); (b) R. A. Mackay and E. J. Paziomek, *ibid.*, **92**, 2432 (1970).

Electron Spin Resonance of Spin Labels in Organic Inclusion Crystals. Models for Anisotropic Motion in Biological Membranes

G. Bruce Birrell, Shui Pong Van, and O. Hayes Griffith*

Contribution from the Institute of Molecular Biology and Department of Chemistry, University of Oregon, Eugene, Oregon 97403. *Received September 6, 1972*

Abstract: Spin labels have been trapped in organic inclusion crystals in order to examine well-defined examples of anisotropic molecular motion. A single crystal 9.5-GHz esr study of di-*tert*-butyl nitroxide (I) in the thiourea host at room temperature has been performed. The spin Hamiltonian is axially symmetric with principal ^{14}N coupling constant and g-value parameters of $A_{||} = 6.2 \pm 0.1$ G, $A_{\perp} = 20.0 \pm 0.1$ G, $g_{||} = 2.0063 \pm 0.0001$, and $g_{\perp} = 2.0059 \pm 0.0001$. The splitting anisotropy equation derived from the spin Hamiltonian, retaining the pseudosecular terms, accounts for the angular dependence of the coupling constant within ± 0.1 G, whereas the first-order treatment accurately predicts the g-value anisotropy. By comparing these data with the rigid lattice parameters, it is established that the spin label I is undergoing rapid, large amplitude motion about the molecular y axis ($\tau < 10^{-8}$ sec, where τ is the rotational correlation time). A line-shape analysis indicates that molecules of I are remarkably well oriented and the angle of tilt is either zero or very nearly zero. Computer simulations establish the acceptable range of orientation parameters as $0 \leq \theta_0 \leq 10°$ and $0 \leq \delta \leq 10°$ where θ_0 and δ are the Gaussian distribution parameter and angle of tilt parameter, respectively. Polycrystalline samples of I in thiourea and 2,2,6,6-tetramethyl-1-oxyl-4-piperidyl dodecanoate (II) in the host β-cyclodextrin are also examined at room temperature and $-196°$. The temperature effects are reversible. At room temperature molecules I and II undergo rapid anisotropic motion about the molecular y axis and x axis, respectively, whereas at $-196°$ the molecules yield rigid glass esr spectra. The effects of x-, y-, and z-axis anisotropic motion on esr spectra of randomly oriented samples are discussed. Esr line shapes calculated assuming anisotropic motion confirm the predicted and experimental results.

Spin labeling is playing an important role in establishing the fluid nature of membrane model systems and biological membranes.[1] The technique consists of incorporating a nitroxide free radical (spin label) into

(1) Recent reviews are: (a) O. H. Griffith and A. S. Waggoner, *Accounts Chem. Res.*, 2, 17 (1969); (b) H. M. McConnell and B. G. McFarland, *Quart. Rev. Biophys.*, 3, 91 (1970); (c) P. Jost, A. S. Waggoner, and O. H. Griffith, "The Structure and Function of Biological Membranes," L. Rothfield, Ed., Academic Press, New York, N. Y., 1971, Chapter 3; (d) I. C. P. Smith, "Biological Applications of Electron Spin Resonance Spectroscopy," J. D. Bolton, D. Borg, and H. Schwartz, Ed., Wiley-Interscience, New York, N. Y., 1972; (e) R. J. Mehlhorn and A. D. Keith in "Molecular Biology of Membranes," C. F. Fox and A. D. Keith, Ed., Sinauer Associates, Stamford, Conn., 1972.

the system of interest and observing the free radical by electron spin resonance (esr). The introduction of steroid[2] and fatty acid[3,4] spin labels has accelerated this work. The lipid spin labels are, of course, asymmetric molecules and tend to undergo molecular motion about preferential directions (*e.g.*, anisotropic motion about the long axis). By using empirical approaches or simple mathematical arguments, it has been possible to draw some conclusions regarding the degree of anisotropic motion.[1] However, progress has been hampered by a lack of unambiguous data on well-defined model systems. Ideally, a model system would possess the following two properties: (1) essentially perfect ordering of the spin labels and (2) a separation of one degree of motional freedom. Phospholipid multilayers[5-8] are perhaps the most relevant model systems because of the almost certain occurrence of bilayers in biological membranes. However, the ordering in phospholipid bilayers and liquid crystals[9-11] is far from perfect and there is usually an admixture of two or more degrees of rotational freedom. A much better choice for the purpose at hand is an organic inclusion compound.

Inclusion compounds are crystalline substances in which two or more components are associated without chemical bonds and in which one of the components fits into cavities formed by the other.[12] Typical hosts are thiourea and urea. X-Ray diffraction studies indicate the cavities formed in these inclusion crystals are hexagonal tubes extending along the sixfold symmetry axis (needle axis) of the crystal.[13-15] The crystals have a honeycomb-like structure and the walls of each cavity are formed by spirals of hydrogen-bonded thiourea or urea molecules. The basic structure is essentially independent of the specific guest molecules trapped in the tubular cavities. The diameters of the cavities are approximately 7 Å for thiourea and 5 Å for urea, placing a restriction on the size and shape of possible guest molecules.[13-15] Generally, urea forms inclusion crystals with straight-chain hydrocarbons while thiourea forms inclusion crystals with certain cyclic and branched-chain hydrocarbons. A number of esr studies have been reported on X-ray produced free radicals derived from guest molecules trapped in organic inclusion compounds.[16] The free radicals are known to orient in the tubular cavities and exhibit a high degree of molecular motion. The picture of an inclusion compound formulated from these studies is that of an extremely well-ordered liquid crystal.

The cyclodextrins form another useful class of inclusion crystals. In this case, the guest molecules fit within the ring-shaped cyclodextrin molecules. The three well-known cyclodextrins are α-, β-, and γ-cyclodextrin. These are composed of six, seven, and eight glucose units, respectively, and have internal diameters of about 6, 8, and 10 Å.[17-19] Our aim is to utilize these inclusion crystals to examine anisotropic motion about the principal axes of nitroxide free radicals. In this paper we report esr studies of di-*tert*-butyl nitroxide (I) and 2,2,6,6-tetramethyl-1-oxyl-4-piperidyl

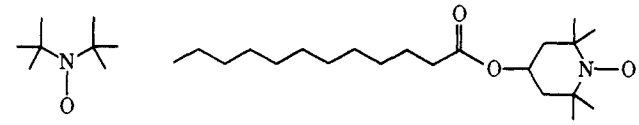

I II

dodecanoate (II) in single crystals of thiourea and polycrystalline β-cyclodextrin, respectively. These results provide unequivocal evidence for y- and x-axis anisotropic motion of spin labels and yield spectral criteria that will be useful in spin labeling studies of biological membranes.

Experimental Section

Di-*tert*-butyl nitroxide was synthesized by the method of Hoffman and Henderson.[20] Single crystals of the I–thiourea inclusion compound were prepared as follows: 0.02 ml of I and 1 ml of 2,2,4-trimethylpentane (isooctane) were added to 5 ml of a saturated solution of thiourea in methanol at 23°, forming a heavy precipitate, methanol was added until the precipitate just dissolved, and the solution was then cooled slowly to 4° over a period of 2 days forming needle-like crystals approximately 1 mm in diameter and 5 mm long.

The lipid spin label II was synthesized by the method of Waggoner, *et al.*[21] Powder samples of the inclusion compound of II with β-cyclodextrin were prepared in the following way: 1.0 mg of II was dissolved in 1 ml of dodecane at 23°, a second solution of 50 mg of β-cyclodextrin dissolved in 1 ml of water at approximately 70° was prepared, and the two solutions were then mixed together forming an immediate precipitate. The precipitate was filtered, washed with hexane, and dried.

The 9.5-GHz esr spectra were recorded using either a Varian E-3 spectrometer or a Varian V-4502 spectrometer. Coupling constants and g values were measured using a Varian V-4532 dual cavity. I (5×10^{-4} M) in 0.01 M phosphate buffer (pH 7.0) at 23° was found to be a convenient standard for coupling constant and g value measurements. Under these conditions the ^{14}N coupling constant of I is 17.16 ± 0.01 G (measured with a Harvey Wells Corp. Model G-502 proton nmr gaussmeter) and $g_0^I = 2.0056 \pm 0.0001$ (relative to the tetracene cation radical, $g = 2.0026$).[22] Within experimental error, a_0^I was found to be constant as the pH was varied between 4 and 9. All ^{14}N coupling constants were determined as one-half the distance in gauss between the high-field and low-field lines.

Simulated esr spectra were generated with a Digital Equipment

(2) J. F. W. Keana, S. B. Keana, and D. Beetham, *J. Amer. Chem. Soc.*, **89**, 3055 (1967).
(3) A. D. Keith, A. S. Waggoner, and O. H. Griffith, *Proc. Nat. Acad. Sci. U. S.*, **61**, 819 (1968).
(4) A. S. Waggoner, T. J. Kingzett, S. Rottschaeffer, O. H. Griffith, and A. D. Keith, *Chem. Phys. Lipids*, **3**, 245 (1969).
(5) L. J. Libertini, A. S. Waggoner, P. C. Jost, and O. H. Griffith, *Proc. Nat. Acad. Sci. U. S.*, **64**, 13 (1969).
(6) J. C. Hsia, H. Schneider, and I. C. P. Smith, *Biochem. Biophys. Acta*, **202**, 399 (1970).
(7) P. Jost, L. J. Libertini, V. C. Hebert, and O. H. Griffith, *J. Mol. Biol.*, **59**, 77 (1971).
(8) B. G. McFarland and H. M. McConnell, *Proc. Nat. Acad. Sci. U. S.*, **68**, 1274 (1971).
(9) H. R. Falle, G. R. Luckhurst, H. Lemaire, Y. Marechal, A. Rassat, and P. Rey, *Mol. Phys.*, **11**, 49 (1966).
(10) P. Ferruti, D. Gill, M. A. Harpold, and M. P. Klein, *J. Chem. Phys.*, **50**, 4545 (1969).
(11) J. Seelig, *J. Amer. Chem. Soc.*, **92**, 3881 (1970).
(12) J. F. Brown, Jr., *Sci. Amer.*, **207** (1), 82 (1962).
(13) A. E. Smith, *Acta Crystallogr.*, **5**, 224 (1952).
(14) H.-U. Lenné, *ibid.*, **7**, 1 (1954).
(15) W. Schlenk, Jr., *Justus Liebigs Ann. Chem.*, **565**, 204 (1949).
(16) (a) O. H. Griffith, *J. Chem. Phys.*, **41**, 1093 (1964); (b) O. H. Griffith, *ibid.*, **42**, 2644 (1965); (c) O. H. Griffith, *ibid.*, **42**, 2651 (1965); (d) O. H. Griffith and M. H. Mallon, *ibid.*, **47**, 837 (1967); (e) O. H. Griffith and E. E. Wedum, *J. Amer. Chem. Soc.*, **89**, 787 (1967); (f) E. E. Wedum and O. H. Griffith, *Trans. Faraday Soc.*, **63**, 819 (1967); (g) G. B. Birrell, A. A. Lai, and O. H. Griffith, *J. Chem. Phys.*, **54**, 1630 (1971); (h) G. B. Birrell, Z. Ciecierska-Tworek, and O. H. Griffith, *J. Phys. Chem.*, **76**, 1819 (1972).
(17) F. Cramer and H. Hettler, *Naturwissenschaften*, **54**, 625 (1967).
(18) D. French, *Advan. Carbohyd. Chem.*, **12**, 189 (1957).
(19) F. R. Senti and S. Erlander, "Nonstoichiometric Compounds," L. Mandelcorn, Ed., Academic Press, New York, N. Y., 1964, p 588.
(20) A. K. Hoffman and A. T. Henderson, *J. Amer. Chem. Soc.*, **83**, 4671 (1961).
(21) A. S. Waggoner, A. D. Keith, and O. H. Griffith, *J. Phys. Chem.*, **72**, 4129 (1968).
(22) B. G. Segal, M. Kaplan, and G. K. Fraenkel, *J. Chem. Phys.*, **43**, 4191 (1965).

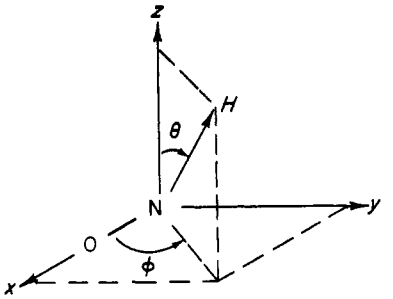

Figure 1. The nitroxide molecular coordinate system and spherical coordinates defining the direction of the laboratory magnetic field (**H**). The molecular x axis lies along the N–O bond, the z axis is parallel to the nitrogen and oxygen 2p orbitals associated with the unpaired electron, and y is perpendicular to the x and z axes.

Corp. PDP-10 computer using the program of Libertini, *et al.*,[5] and were plotted on a Houston Instrument 2000 recorder or a Cal-Comp plotter.

Results and Discussion

1. Spin Hamiltonian. Nitroxide free radicals oriented in a crystalline matrix are characterized by the spin Hamiltonian

$$\hat{\mathcal{H}} = \beta_e \mathbf{H}\cdot\mathbf{g}\cdot\hat{\mathbf{S}} + \hat{\mathbf{S}}\cdot\mathbf{A}\cdot\hat{\mathbf{I}} \qquad (1)$$

where β_e, **H**, **g**, **A**, $\hat{\mathbf{S}}$, and $\hat{\mathbf{I}}$ are the electron Bohr magneton, the laboratory magnetic field vector, the g value matrix, hyperfine matrix, the electron spin operator, and the ^{14}N nuclear spin operator, respectively. A detailed discussion of this Hamiltonian for nitroxide free radicals, including an experimental and theoretical justification for the neglect of the nuclear Zeeman term, has been published elsewhere.[2,3] The esr spectrum of an oriented ensemble of nitroxide free radicals consists of three lines, separated by the hyperfine splitting A and centered at a field (H) defined by the g value parameter. The principal axes of the **A** and **g** tensors essentially coincide and together define the molecular axes system x, y, z shown in Figure 1. The principal g values and splittings g_{xx}, g_{yy}, g_{zz} and A_{xx}, A_{yy}, A_{zz} measured along these three directions are a property of the paramagnetic RR'N–O group and vary only slightly with the structure of the nitroxide and the polarity of the environment. The largest splitting A_{zz} is typically 31–33 G and the smallest splitting is $A_{xx} \simeq A_{yy} \simeq 6$ G.

In their study of di-*tert*-butyl nitroxide oriented in single crystals of tetramethyl-1,3-cyclobutanedione, Libertini and Griffith compared the exact solution of the spin Hamiltonian with the experimental esr data and with various approximate analytical expressions.[2,3] In terms of the usual spherical coordinates relating the magnetic field vector to the molecular coordinate system (see Figure 1), the orientation dependence of g and A at 9.5 GHz is accurately given by the equations

$$g(\theta,\phi) = g_{xx}\sin^2\theta\cos^2\phi + g_{yy}\sin^2\theta\sin^2\phi + g_{zz}\cos^2\theta \qquad (2)$$

$$A(\theta,\phi) = \{A_{xx}^2\sin^2\theta\cos^2\phi + A_{yy}^2\sin^2\theta\sin^2\phi + A_{zz}^2\cos^2\theta\}^{1/2} \qquad (3)$$

A less accurate but very useful relation for A is

$$A(\theta,\phi) = A_{xx}\sin^2\theta\cos^2\phi + A_{yy}\sin^2\theta\sin^2\phi + A_{zz}\cos^2\theta \qquad (4)$$

(23) L. J. Libertini and O. H. Griffith, *J. Chem. Phys.*, **53**, 1359 (1970).

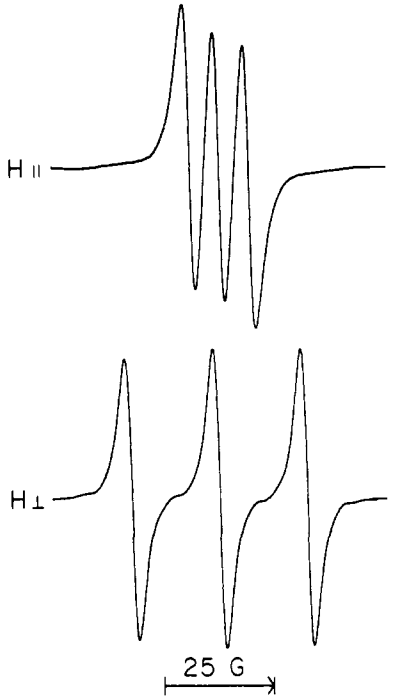

Figure 2. Room-temperature esr spectra of di-*tert*-butyl nitroxide trapped in a single crystal of thiourea, recorded at the two principal crystalline orientations. $H_{||}$ and $H_{\perp}$ indicate the direction of the magnetic field with respect to the crystalline needle axis.

furthermore, if the hyperfine Hamiltonian is taken to be strictly axially symmetric, *i.e.*, if $A_{xx} = A_{yy}$, eq 3 and 4 reduce to

$$A(\theta) = \{A_{xx}^2\sin^2\theta + A_{zz}^2\cos^2\theta\}^{1/2} \qquad (5)$$

and

$$A(\theta) = A_{xx}\sin^2\theta + A_{zz}\cos^2\theta \qquad (6)$$

Equations 3 and 5 take into account pseudosecular terms ($\hat{S}_z\hat{I}_z$, $\hat{S}_z\hat{I}_y$) in the Hamiltonian (eq 1), whereas eq 4 and 6 are first-order treatments that retain only the secular ($\hat{S}_z\hat{I}_z$) hyperfine interaction term.

2. Esr Spectral Anisotropy in Single Crystals Exhibiting y-Axis Anisotropic Motion. Esr spectra of di-*tert*-butyl nitroxide in thiourea were recorded at 10° intervals as the crystals were rotated in the magnetic field. The smallest splitting is observed with **H** parallel to the needle axis (z' axis), and the largest splitting is observed with **H** in the $x'y'$ plane of the hexagonal crystal (see Figure 2). *However, the spectrum is invariant with respect to rotations of the magnetic field in the $x'y'$ plane.* This effect can only arise from (1) random free radical orientations in the $x'y'$ plane, (2) accidental isotropic magnetic interactions in the $x'y'$ plane, or (3) rapid large amplitude motion in the crystalline $x'y'$ plane. The first possibility is clearly ruled out by the sharp symmetrical three-line spectrum. We shall now show that the second possibility is not the case, and in fact *di-tert-butyl nitroxide undergoes almost perfect y-axis anisotropic motion in the thiourea matrix.*

In order to analyze the effects of molecular motion it is convenient to choose a laboratory coordinate system (x', y', z') with the z' axis parallel to **H**. The appropriate coordinate transformation matrix, **L**, required to transform a vertical vector **r** from the un-

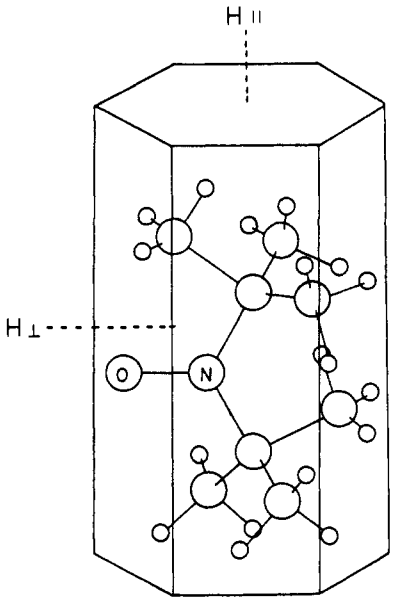

Figure 3. A schematic diagram showing one orientation of a di-*tert*-butyl nitroxide molecule inside the thiourea hexagonal crystalline matrix.

primed (molecular) to the primed (laboratory) coordinate system is

$$\mathbf{L} = \begin{pmatrix} \cos\theta\cos\phi & \cos\theta\sin\phi & -\sin\theta \\ -\sin\phi & \cos\phi & 0 \\ \sin\theta\cos\phi & \sin\theta\sin\phi & \cos\theta \end{pmatrix} \quad (7)$$

where θ and ϕ are the usual spherical coordinates. The Hamiltonian of eq 1 is a scalar quantity and must be invariant to a unitary transformation. It follows that

$$\mathcal{H} = \beta_e(\mathbf{H}\cdot\mathbf{L}^\tau)\cdot(\mathbf{L}\cdot\mathbf{g}\cdot\mathbf{L}^\tau)\cdot(\mathbf{L}\cdot\hat{\mathbf{S}}) + (\hat{\mathbf{S}}\cdot\mathbf{L}^\tau)\cdot(\mathbf{L}\cdot\mathbf{A}\cdot\mathbf{L}^\tau)\cdot(\mathbf{L}\cdot\hat{\mathbf{I}}) \quad (8)$$

or

$$\mathcal{H} = \beta_e\mathbf{H}'\cdot\mathbf{g}'\cdot\hat{\mathbf{S}}' + \hat{\mathbf{S}}'\cdot\mathbf{A}'\cdot\hat{\mathbf{I}}' \quad (9)$$

where

$$\mathbf{g}' = \mathbf{L}\cdot\mathbf{g}\cdot\mathbf{L}^\tau \text{ and } \mathbf{A}' = \mathbf{L}\cdot\mathbf{A}\cdot\mathbf{L}^\tau \quad (10)$$

since from matrix mechanics $\mathbf{L}\cdot\mathbf{r} = \mathbf{r}'$, $\mathbf{r}^\tau\cdot\mathbf{L}^\tau = \mathbf{r}'^\tau$, and $\mathbf{L}\cdot\mathbf{L}^\tau = \mathbf{L}^\tau\cdot\mathbf{L} = \mathbf{I}$, where τ denotes transpose and $\mathbf{I}$ is the identity matrix.[23,24]

Performing the transformation and retaining only the terms found to be significant by Libertini and Griffith[23] gives

$$\mathcal{H} = \beta\{(g_{xx}\cos^2\phi + g_{yy}\sin^2\phi)\sin^2\theta + g_{zz}\cos^2\theta\}H\hat{S}_{z'} + \{(A_{xx}\cos^2\phi + A_{yy}\sin^2\phi)\times \sin^2\theta + A_{zz}\cos^2\theta\}\hat{S}_{z'}\hat{I}_{z'} + \{(A_{xx}\cos^2\phi + A_{yy}\sin^2\phi - A_{zz})\sin\theta\cos\theta\}\hat{S}_{z'}\hat{I}_{x'} + \{(-A_{xx} + A_{yy})\sin\theta\sin\phi\cos\phi\}\hat{S}_{z'}\hat{I}_{y'} \quad (11)$$

If the magnetic field is now directed along the molecular y axis, $\theta = 90°$, $\phi = 90°$, and $\mathcal{H}$ becomes

$$\mathcal{H} = \beta g_{yy}H\hat{S}_{z'} + A_{yy}\hat{S}_{z'}\hat{I}_{z'} \quad (12)$$

(24) L. J. Libertini, Ph.D. Dissertation, University of Oregon, 1971.

whereas with $\mathbf{H}$ in the molecular xz plane, $\phi = 0°$, and

$$\mathcal{H} = \beta(g_{xx}\sin^2\theta + g_{zz}\cos^2\theta)H\hat{S}_{z'} + (A_{xx}\sin^2\theta + A_{zz}\cos^2\theta)\hat{S}_{z'}\hat{I}_{z'} + (A_{xx} - A_{zz})\sin\theta\cos\theta\,\hat{S}_{z'}\hat{I}_{x'} \quad (13)$$

Equation 12 contains no angular terms and is invariant to molecular motion in the xy plane. The solution is, as expected, a three line esr spectrum characterized by the parameters g_{yy} and A_{yy}. However, eq 13 contains angular-dependent terms and the nature of the motion must be specified. We now assume that (1) the motion is rapid, *i.e.*, $\tau \ll |(A_{zz} - A_{xx})^{-1}| \sim 10^{-8}$ sec, where A_{zz} and A_{xx} are expressed in frequency units and τ is the rotational correlation time, and (2) the motion is of large amplitude (*ca.* >90°) or is simply rotation about the y axis. Under these conditions θ represents an angle between a fixed direction ($\mathbf{H}$) in space and rapidly tumbling molecular axes. During a time interval on the order of τ, the molecular x and z axes will point with equal probability through all equal arcs on the circumference of a unit circle and the mean values of the angular-dependent terms become

$$\overline{(g_{xx}\sin^2\theta + g_{zz}\cos^2\theta)} = \frac{1}{2\pi}\int_0^{2\pi}(g_{xx}\sin^2\theta + g_{zz}\cos^2\theta)\,d\theta = \frac{1}{2}(g_{xx} + g_{zz}) \quad (14)$$

likewise

$$\overline{A_{xx}\sin^2\theta + A_{zz}\cos^2\theta} = (1/2)(A_{xx} + A_{zz}) \quad (15)$$

and

$$\overline{(A_{xx} - A_{zz})\sin\theta\cos\theta} = \frac{1}{2\pi}(A_{xx} - A_{zz})\int_0^{2\pi}\sin\theta\cos\theta\,d\theta = 0 \quad (16)$$

Substituting these averages into eq 13 and solving yields a three line esr spectrum characterized by the average A and g values.

To summarize, rapid molecular motion about the y molecular axis reduces the Hamiltonian to an axially symmetric form and the principal values $A_{||}$, $g_{||}$ and $A_\perp$, $g_\perp$ are

$$A_{||} = A_{yy} \quad (17)$$

$$g_{||} = g_{yy} \quad (18)$$

$$A_\perp = (1/2)(A_{xx} + A_{zz}) \quad (19)$$

$$g_\perp = (1/2)(g_{xx} + g_{zz}) \quad (20)$$

Similar equations apply for rotation about other axes. The equations are accurate in that they are derived from a Hamiltonian containing the pseudosecular terms. Formally, the same results can be obtained from the first-order anisotropy term, eq 6. This is fortuitous and eq 5 does not yield the correct average even though it was derived retaining the pseudosecular terms.[23] The correct method is to average the Hamiltonian and not the final anisotropy equations. The equations for $A_{||}$, $g_{||}$ and $A_\perp$, $g_\perp$ have been used for some time in interpreting esr spectra of X-ray produced free radicals in urea inclusion compounds.[16]

The principal values for di-*tert*-butyl nitroxide oriented in tetramethyl-1,3-cyclobutanedione at room temperature are A_{xx} = 7.6 G, A_{yy} = 6.0 G, A_{zz} = 31.8 G and g_{xx} = 2.0088, g_{yy} = 2.0062, g_{zz} = 2.0027.[23]

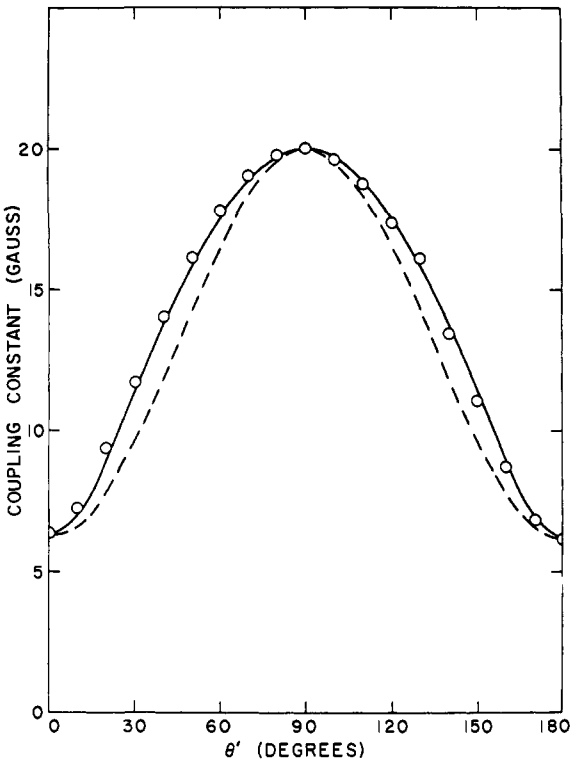

Figure 4. Angular variation of the coupling constant of di-*tert*-butyl nitroxide included in thiourea with the direction of the magnetic field at room temperature. The open circles are experimental points. The solid line is the theoretical curve of eq 5 and the dashed line is the theoretical curve of eq 6. θ' is the angle between the direction of the magnetic field and the needle axis of the thiourea crystal.

Using eq 17 and 19, the calculated values for rapid molecular motion about the y axis become $A_{||} = A_{yy} =$ 6.0 G and $A_{\perp} = (1/2)(A_{xx} + A_{zz}) = 19.7$ G. These values are in excellent agreement with the observed data $A_{||} = 6.2 \pm 0.1$ G and $A_{\perp} = 20.0 \pm 0.1$ G. Likewise, the expected g values for y-axis anisotropic motion are $g_{||} = g_{yy} = 2.0062$ and $g_{\perp} = (1/2)(g_{xx} + g_{zz}) =$ 2.0057. These numbers are equal, within experimental error, to the observed quantities $g_{||} = 2.0063 \pm 0.0001$ and $g_{\perp} = 2.0059 \pm 0.0001$. From these data, we conclude that the di-*tert*-butyl nitroxide free radical is aligned as shown in Figure 3. The molecular y axis lies very nearly along the crystalline z' axis and the N–O group is undergoing rapid large amplitude oscillations (or rotation) in the crystalline $x'y'$ plane.

The complete room temperature anisotropy of the splitting and g value are given as open circles in Figures 4 and 5, where θ' is the angle between **H** and the crystalline needle axis. According to the theory, the hyperfine anisotropy may be calculated from eq 5 and 6 using the observed motion-averaged principal values $A_{||}$ and $A_{\perp}$ in place of A_{xx} and A_{zz}. These two curves are shown in Figure 4 as solid and dashed lines, respectively. Equation 5 provides a better fit to the experimental curve as expected, but eq 6 is sufficiently accurate to be useful. In Figure 5, the solid line is a plot of $g(\theta) = g_{\perp} \sin^2 \theta + g_{||} \cos^2 \theta$ where $g_{\perp} = 2.0059$ and $g_{||} = 2.0063$. This expression provides an excellent fit to the experimental g-value data of Figure 5, and this concludes our description of the room-temperature esr spectral anisotropy of di-*tert*-butyl nitroxide in the thiourea host crystal.

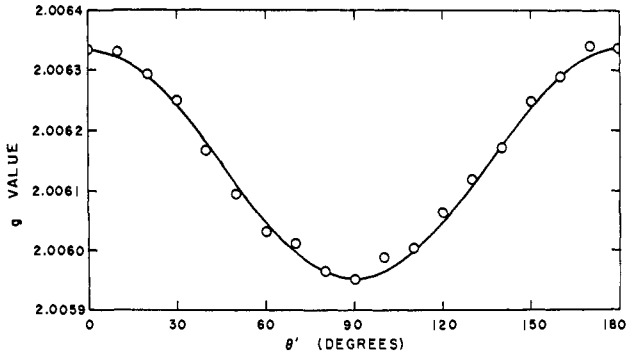

Figure 5. Angular variation of the g value of di-*tert*-butyl nitroxide included in thiourea with the direction of the magnetic field at room temperature. The open circles are experimental points. The solid line is the theoretical curve of eq 2. θ' is the angle between the direction of the magnetic field and the needle axis of the thiourea crystal.

3. Line-Shape Analysis of the Single Crystal Data. It is instructive to examine the line shapes in terms of the orientation distribution treatment introduced by Libertini, *et al.*, in studies of phospholipid multilayers.[5] In this approach the ensemble of spin labels are no longer oriented perfectly in the sample. Instead, the long axes (R) are assumed to exist in a Gaussian distribution of orientations. The probability of finding R between θ and $\theta + d\theta$ is given by the Gaussian distribution function $\sin\theta \exp\{-2(\theta - \delta)^2/\theta_0^2\}$, where θ is the angle between R and the crystalline z' axis, δ is the most probable orientation measured from the z' axis, and θ_0 is a measure of degree of order of the system. The two parameters θ_0 and δ are referred to as the Gaussian distribution parameter and the angle of tilt, respectively. The two parameters are independent but, as pointed out previously (see footnote 13 of ref 5), it is difficult to distinguish the effects of a very small angle of tilt. The normal practice is to establish ranges or upper limits of δ and θ_0 by comparing computer simulated spectra with the experimental spectra.

The computer program has been described elsewhere.[5,24] The input data in the absence of molecular motion include the microwave frequency, the field direction, the number of spin labels in the ensemble (*i.e.*, 2000), the principal values A_{xx}, A_{yy}, A_{zz}, and g_{xx}, g_{yy}, g_{zz}, a choice of esr line shape (*e.g.*, Gaussian or Lorentzian), and the two parameters of interest, θ_0 and δ. Introducing the effects of molecular motion is simple, providing the motion is rapid, that is, if $\tau < (A_{zz} - A_{xx})^{-1} \simeq 10^{-8}$ sec, where A_{zz} and A_{xx} are expressed in frequency units and τ is the rotational correlation time. In our case A_{xx}, A_{zz} and g_{xx}, g_{zz} may be replaced by the motion averaged values $A_{\perp} = (1/2)\cdot(A_{xx} + A_{zz})$ and $g_{\perp} = (1/2)(g_{xx} + g_{zz})$ as discussed above. Figure 6 shows a trial calculation to establish whether the line shapes are Gaussian or Lorentzian. By comparing Figure 6 with Figure 2 it is clear that the individual esr lines are more nearly Lorentzian. This was confirmed in simulations using other input parameters (*e.g.*, θ_0, δ, and line widths).

The effect of varying θ_0 is shown in Figure 7. The limit $\theta_0 \to 0$ represents perfect crystalline order and $\theta_0 \to \infty$ corresponds to a completely random sample. Comparing Figures 7 and 2 places an upper limit of about 10° on θ_0. Larger values of θ_0 introduce line

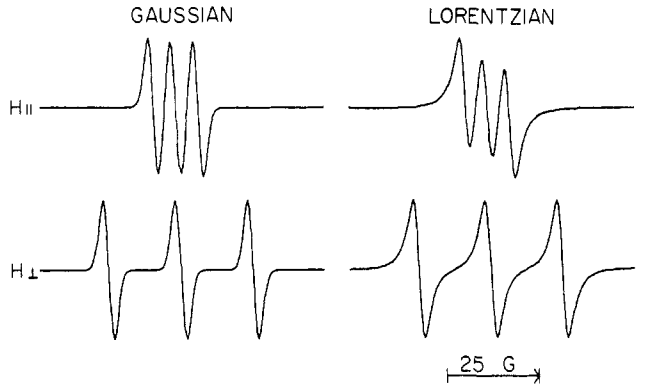

Figure 6. Effects of variations in line shape on computer simulations of the esr spectra of Figure 2. $H_{\parallel}$ and $H_{\perp}$ indicate the direction of the magnetic field with respect to the crystalline needle axis. Coupling constants and g values used in the simulations were $A_{\parallel} = A_{yy} = 6.2$ G, $g_{\parallel} = g_{yy} = 2.0063$ and $A_{\perp} = (1/2)(A_{xx} + A_{zz}) = 20.0$ G, $g_{\perp} = (1/2)(g_{xx} + g_{zz}) = 2.0059$. A distribution width ($\theta_0$) of 5° and a line width of 3.0 G were used in each of the simulations.

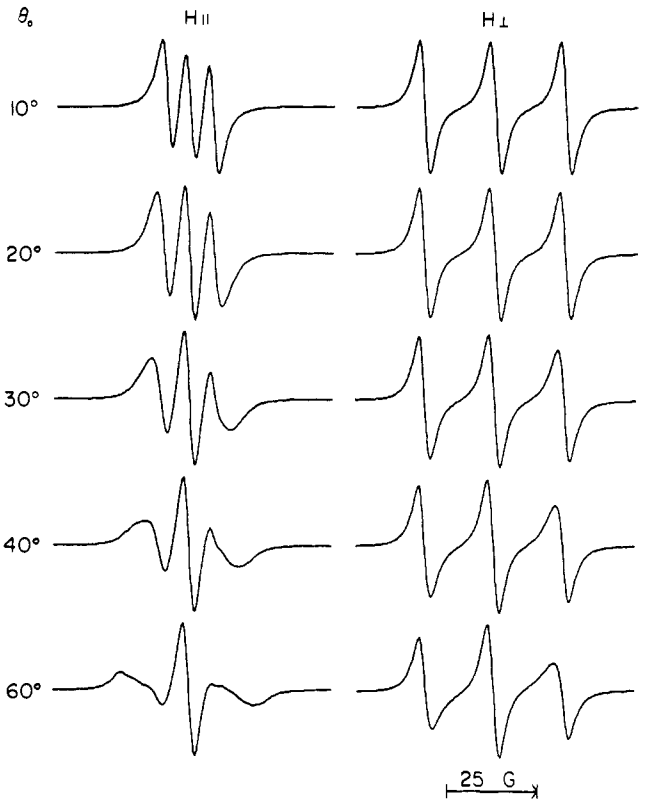

Figure 7. Effects of varying the distribution width, θ_0, of the oriented nitroxides on computer simulations of the esr spectra of di-*tert*-butyl nitroxide of Figure 2. $H_{\parallel}$ and $H_{\perp}$ indicate the direction of the magnetic field with respect to the crystalline needle axis. Coupling constants and g values used in each of the simulations are the same as in Figure 6. The line width was 3.0 G for each simulation; the line shape chosen was Lorentzian.

broadening, particularly in the $H_{\parallel}$ spectrum, that is not consistent with the experimental data of Figure 2. The maximum angle of tilt is also small (see Figure 8). Increasing δ has the effect of increasing $A_{\parallel}$ and decreasing $A_{\perp}$. Computer simulations establish the acceptable range of parameters as $0 \leq \theta_0 \leq 10°$ and $0 \leq \delta \leq 10°$. Evidently the y axes of di-*tert*-butyl nitroxide molecules are as well oriented in thiourea as they are in the semirigid matrix, tetramethyl-1,3-cyclobutanedione. This is remarkable in view of the fact

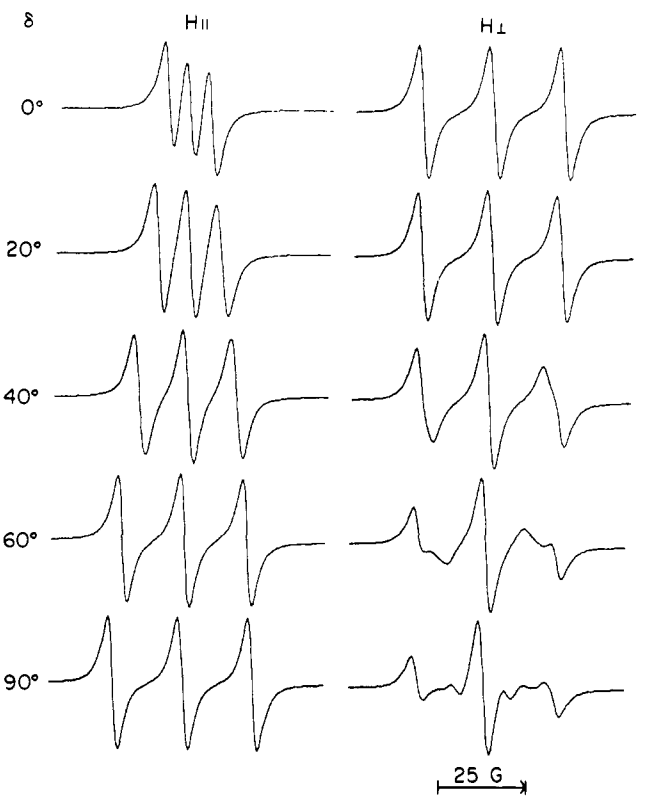

Figure 8. Effects of varying the angle of tilt, δ, on computer simulations of the esr spectra of di-*tert*-butyl nitroxide of Figure 2. Coupling constants and g values used in each of the simulations are the same as in Figure 6. A distribution width (θ_0) of 5° and a line width of 3.0 G were used in each of the simulations; the line shape chosen was Lorentzian.

that di-*tert*-butyl nitroxide is very nearly spherical in shape and is undergoing large amplitude motion in the tubular cavities of thiourea. Heating the thiourea inclusion crystal from room temperature to the point at which the signal decays (~80°) produces no marked changes in the esr spectra of Figure 2.

4. Recognizing Anisotropic Motion in Polycrystalline Samples. (A) Anisotropic Motion about the x Axis. In proceeding from a single crystal to a polycrystalline sample there is a loss of information and it is more difficult to interpret the esr spectra. The polycrystalline sample may exhibit various types of anisotropic molecular motion (or even isotropic motion) depending on the geometry of the spin label and the nature of the host. Thus, the word polycrystalline as it is used here indicates random orientation with respect to **H** but carries no implications regarding the mobility of the spin labels. If the polycrystalline samples are cooled to a sufficiently low temperature, all spectra will approach the rigid matrix limit (generally referred to as rigid glass whether it is a glass, polycrystalline sample, or biological specimen). There are small variations in rigid glass spectra caused by differences in polarity of the environment and intrinsic line widths, but the general line shape is easily recognized. In Figure 9, spectrum a is the rigid glass line shape obtained by cooling the polycrystalline sample of di-*tert*-butyl nitroxide in thiourea to −196°. The rigid glass spectrum is a superposition of esr spectra from all possible orientations of spin labels and the distance between the outermost lines is $2A_{zz}$ (see eq 5 or 6).

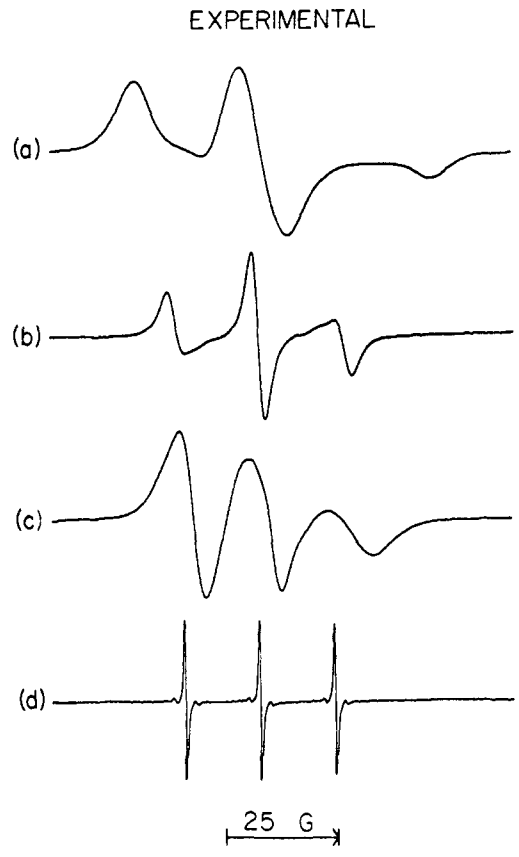

Figure 9. Experimental esr spectra of randomly oriented nitroxides: (a) di-*tert*-butyl nitroxide trapped in thiourea at −196°; (b) di-*tert*-butyl nitroxide trapped in thiourea at 24°; (c) 2,2,6,6-tetramethyl-1-oxyl-4-piperidyl dodecanoate (II) trapped in β-cyclodextrin at 24°; (d) solution spectrum of di-*tert*-butyl nitroxide in water at 24°.

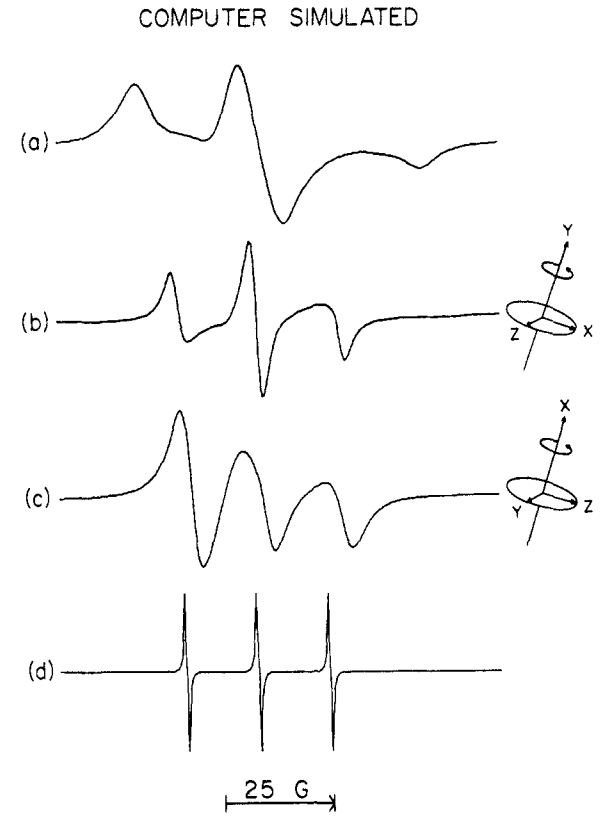

Figure 10. Computer simulations of the esr spectra of Figure 9: (a) computed spectrum for a randomly oriented collection of rigid nitroxides; (b) the corresponding spectrum allowing rotation about the y axis only; (c) the result for rotation about the x axis only; (d) the spectrum assuming rapid rotation about all three molecular axes. Coupling constants and g values used in the simulations were: (a) A_{xx} = 7.6 G, A_{yy} = 6.0 G, A_{zz} = 33.9 G, g_{xx} = 2.0088, g_{yy} = 2.0062, g_{zz} = 2.0027; (b) $A_{||}$ = 6.2 G, $g_{||}$ = 2.0062, $A_{\perp} = (1/2)\cdot(A_{xx} + A_{zz})$ = 20.0 G, $g_{\perp} = (1/2)(g_{xx} + g_{zz})$ = 2.0059; (c) $A_{||} = A_{xx}$ = 7.6 G, $g_{||} = g_{xx}$ = 2.0088, $A_{\perp} = (1/2)(A_{yy} + A_{zz})$ = 18.9 G, $g_{\perp} = (1/2)(g_{yy} + g_{zz})$ = 2.0044; (d) A = 17.2 G, g = 2.0059. Line widths (G) were (a) 6.0; (b) 3.0; (c) 5.0; (d) 0.4. The line shape chosen was Lorentzian, and θ_0 = 10,000 for all computer simulations of this figure. Because of the random orientations, the angle of tilt parameter, δ, has no effect on the computer simulations of polycrystalline esr data.

The three types of anisotropic motion central to this discussion are rapid large amplitude motion about the x, y, or z nitroxide axes. Consider first anisotropic motion about the x axis. Following the above arguments the Hamiltonian now has axial symmetry and the two principal esr spectra are characterized by $A_{||}$, $g_{||}$ and $A_{\perp}$, $g_{\perp}$, respectively, where $A_{||} = A_{xx}$ = 7.6 G, $g_{||} = g_{xx}$ = 2.0088, $A_{\perp} = (1/2)(A_{yy} + A_{zz}) = (1/2)(6.0 + 31.8)$ = 18.9 G, and $g_{\perp} = (1/2)(g_{yy} + g_{zz}) = (1/2)\cdot(2.0062 + 2.0027)$ = 2.0044. The polycrystalline spectrum is a superposition of these two principal spectra plus spectra at intermediate orientations of the magnetic field. The maximum splitting in the conventional 9.5-GHz experiment will be on the order of 2 × 18.9 = 37.8 G, and the spectrum will be very asymmetric owing to the large difference in $g_{||}$ and $g_{\perp}$. Furthermore, the high-field line will have the lowest intensity because $g_{||} > g_{\perp}$, shifting the $A_{||}$, $g_{||}$ spectrum downfield. The polycrystalline sample of II in β-cyclodextrin provides a probable example of x-axis anisotropic motion. The x axis is parallel to the long axis of the spin label and the β-cyclodextrin tends to restrict motion other than oscillations or rotations about the long axis. Spectrum c in Figure 9 is the room-temperature esr spectrum. The overall splitting and general appearance of this spectrum are consistent with x-axis anisotropic motion. An interesting feature is the decrease in peak heights proceeding from the low- to high-field lines. Upon cooling, this spectrum approaches a typical rigid glass line shape and the effect is reversible. Mehlhorn and Keith[16] have recently observed the same spectral features using a molecule very similar to II dispersed in asolectin at 30°. On the basis of Monte Carlo simulations, these authors conclude that the main features of the esr spectra can be accounted for in terms of rapid anisotropic motion about the x axis.

(B) Anisotropic Motion about the y Axis. Motion about the y axis is the best documented example of anisotropic motion because of the new single crystal esr data on di-*tert*-butyl nitroxide in the thiourea host (Figure 2). If these crystals are ground into a fine polycrystalline sample, spectrum b of Figure 9 is observed at room temperature. As discussed above, the two principal spectral components are characterized by $A_{||} = A_{yy}$ = 6.0 G, $g_{||} = g_{yy}$ = 2.0062 and $A_{\perp} = (1/2)\cdot(A_{xx} + A_{zz})$ = 19.7 G, $g_{\perp} = (1/2)(g_{xx} + g_{zz})$ = 2.0057. The maximum splitting in the polycrystalline spectrum is, therefore, predicted to be on the order of 2 × 19.7 = 39 G. The spectrum will be very nearly symmetrical about the center since $g_{||} \sim g_{\perp}$, and for the same reason, the intensity of the center line must be greater than the

outer lines. In Figure 9, the overall splitting of spectrum c is ~37 G and the expected symmetry and apparent relative intensities are also observed. If the sample is cooled to −196°, the esr spectrum reversibly becomes Figure 9a. Evidence of molecular motion about the y axis has been obtained and discussed previously by Hubbell and McConnell,[25] Hsia, Schneider, and Smith,[6] and Mehlhorn and Keith.[1e] These discussions and data are consistent with the single crystal and polycrystalline data presented here.

(C) Anisotropic Motion about the z Axis. Motion about the z axis averages the x and y components so that $A_{||} = A_{zz} = 31.8$ G, $g_{||} = g_{zz} = 2.0027$, $A_{\perp} = (1/2)(A_{xx} + A_{yy}) = (1/2)(6.0 + 7.6) = 6.8$ G, and $g_{\perp} = (1/2)(g_{xx} + g_{yy}) = (1/2)(2.0088 + 2.0062) = 2.0075$. There is no effect on the maximum splitting ($2 \times 31.8 = 63.6$ G) at 9.5 GHz and practically no effect on the small principal splitting since $A_{xx} \sim A_{yy}$. The averaging of g_{xx} and g_{yy} is more significant. Since $g_{\perp} > g_{||}$, any observable effects will occur on the low-field side of the center line. In summary, the conventional 9.5-GHz spectrum of a spin label rapidly rotating about the z nitroxide axis will resemble the rigid glass spectrum with some minor line-shape differences on the low-field side of the spectrum. Evidence for z-axis anisotropic motion from conventional 9.5-GHz esr experiments is, therefore, not conclusive, and we have not attempted to include examples in this paper. Fortunately, the situation at higher microwave frequencies is more promising. *At 35 GHz, for example, the g-factor shifts are sufficiently large that the overall splitting in the rigid glass is no longer $2A_{zz}$.* Instead, it is a function of A_{zz}, A_{xz}, g_{zz}, and g_{xz} and will be affected by anisotropic motion about the z axis. A study of anisotropic motion at 35 GHz is in progress and it will be interesting to compare 35- and 9.5-GHz data.

(25) W. L. Hubbell and H. M. McConnell, *Proc. Nat. Acad. Sci. U. S.*, **63**, 16 (1969).

(D) Line-Shape Simulations. Computer simulations provide a convenient check on the qualitative discussion of x, y, and z anisotropic motion in randomly oriented samples. In Figure 10, a is a computed rigid glass spectrum, b is a spectrum calculated assuming rapid motion about the y axis, c is a spectrum calculated for motion about the x axis, and d is a simulation of rapid isotropic tumbling included as a reference. The corresponding spectrum calculated for motion about the z axis resembles in most respects the rigid glass spectrum a and is not shown. (A figure similar to Figure 10 appears in ref 1c, as part of a general review of anisotropic motion.) All of the spectra of Figure 10 were computed using the program of Libertini, *et al.*,[5,24] with $\theta_0 = 10{,}000$ to ensure random orientation. Increasing θ_0 beyond 10,000 did not cause significant line-shape changes. The motion-averaged A and g parameters used were those discussed above. A comparison of the computed spectra of Figure 10 with the corresponding experimental esr spectra of Figure 9 shows excellent agreement. The only parameter varied to achieve this fit was the intrinsic line width, and in no case did reasonable line width variations change the basic features of the spectra. It should be emphasized that these experimental and simulated esr spectra represent the limits of complete averaging of the tensor elements in one principal plane arising from rotation (or large amplitude motion) about the x, y, or z axis of the nitroxide. Restricted oscillations about one axis can also occur and yield line shapes intermediate between the limiting cases of large amplitude anisotropic motion and the single crystal or rigid glass spectra.

Acknowledgment. We are pleased to acknowledge useful discussions with Dr. Patricia Jost and T. Marriott. We also gratefully acknowledge the Corn Products Co. for the sample of β-cyclodextrin. This work was supported by U. S. Public Health Service Grant CA 10337 from the National Cancer Institute.